Available online at www.sciencedirect.com
ScienceDirect
Journal of Magnetic Resonance 189 (2007) 200–208
JMR Journal of Magnetic Resonance
www.elsevier.com/locate/jmr

# Simulation of steady-state NMR of coupled systems using Liouville space and computer algebra methods

Christopher Kumar Anand [a], Alex D. Bain [b,*], Zhenghua Nie [c]

[a] Department of Computing and Software, McMaster University, 1280 Main Street West, Hamilton, ON, Canada L8S 4K1
[b] Department of Chemistry, McMaster University, 1280 Main Street West, Hamilton, ON, Canada L8S 4M1
[c] School of Computational Engineering and Science, McMaster University, 1280 Main Street West, Hamilton, ON, Canada L8S 4K1

Received 26 May 2007; revised 3 September 2007
Available online 20 September 2007

**Abstract**

A series of repeated pulses and delays applied to a spin system generates a steady state. This is relatively easy to calculate for a single spin, but coupled systems present real challenges. We have used Maple, a computer algebra program to calculate one- and two-spin symbolically, and larger systems numerically. The one-spin calculations illustrate and validate the methods and show how the steady-state free precession method converges to continuous wave NMR. For two-spin systems, we have derived a general formula for the creation of double-quantum signals as a function of irradiation strength, coupling constant, and chemical shift difference. The calculations on three-spin and larger systems reproduce and extend previously published results. In this paper, we have shown that the approach works well for systems in literature. However, the formalism is general and can be extended to more complex spin systems and pulses sequences.


*Keywords:* Steady state; Pulsed NMR; Continuous wave NMR; Multiple quantum transitions; Liouville space methods; Computer algebra program

## 1. Introduction

This paper develops an approach to steady-state methods for creating "interesting" spin density matrices. Most current NMR experiments start with the density matrix at equilibrium and manipulate it with a series of pulses and delays [1–3]. However, non-selective pulses and J-couplings can be somewhat crude tools for this work. Steady-state methods offer an alternative approach [4]. In this case, the effect of a repeated pulse sequence is balanced against relaxation until a steady state is achieved. This has clear analogies to CW methods [5–7]. Steady-state methods can create otherwise-inaccessible states of the spin system. Furthermore, data can be acquired more quickly, since there are no relaxation delays. This technique has been relatively little explored in the general case of non-trivial pulse sequences and complex spin systems.

Solving for this steady state requires a different set of tools from standard product–operator methods, particularly because relaxation is a necessary part of the calculation. Computer algebra methods, such as Maple or Mathematica are extremely helpful [8–14]. They efficiently provide correct and lucid symbolic solutions to the simpler cases, and reliable numerical solutions for systems in which the algebra gets out of hand. In this paper we explore steady-state solutions for a single spin-$\frac{1}{2}$ and systems of coupled spins.

Steady-state methods are not new. Carr described the steady-state free-precession (SSFP) method in 1958 [4]. Artifacts from fast pulsing in Fourier transform NMR were recognized as steady-state effects by Freeman and Hill [15] and more general steady states were analyzed [16]. More recently, steady-state methods in medical imaging have led to much faster acquisitions, even real-time imaging [17–21]. Since the bulk of this work is aimed at anatomical

* Corresponding author. Fax: +1 905 522 2509.
*E-mail address:* bain@mcmaster.ca (A.D. Bain).

1090-7807/$ - see front matter © 2007 Elsevier Inc. All rights reserved.
doi:10.1016/j.jmr.2007.09.012

or relaxation-weighted images, most of the analysis of steady-state experiments has been based on a system of a single spin-$\frac{1}{2}$, which can be described by the Bloch equations. Some researchers have looked at steady states of coupled spin systems, but the driving force was simply CW irradiation. Complete descriptions of steady-state methods are not available in literature. In this paper, we provide a general formalism for dealing with any spin system subjected to any pulse sequence. The purpose here is to establish the approach, and future work will present some of the applications.

In order to validate this formalism, we explore some of the published cases. An important example is the SSFP method [4,22,23]. In this case, the excitation consists of a series of identical rf pulses, followed by delays. In the limit of short delays, this becomes equivalent to CW irradiation with the time-averaged rf power. We show that our formalism not only reproduces the CW limit, but also shows what happens when the SSFP approximation breaks down. A more modern example is the direct creation of multiple-quantum coherence [5,6,24,25]. Strong CW irradiation of coupled spin systems can produce signals at multiple-quantum frequencies. An approximate symbolic solution for two coupled spins is available in literature [26], which we are able to reproduce and extend with a Maple derivation. Finally, Worvill [7] used saturating CW rf as a way of probing spin relaxation in coupled spin systems. This presents a challenging problem, since it tests all aspects of our method: the description of the spin system, the description of the irradiation and the description of relaxation. We have repeated this calculation numerically, using a simpler model of relaxation, and have reproduced the general features of the published spectra. Since we use a Liouville space method, incorporating more sophisticated relaxation mechanisms is straightforward, but not essential to validating our formalism.

A formalism does more than simply describing an experiment, it also provides a method for optimizing it. The results from a steady-state calculation may not be intuitively clear or easy to picture. Therefore, modern optimization methods can be very useful in fine-tuning a steady-state method. Computer algebra can be of great benefit here, since it can provide derivatives with respect to experimental parameters. We have done some preliminary work on this [27], and future papers will explore this aspect as well. In this paper, we present and validate a general formalism for describing steady-state methods and hope this work will renew interest in this technique.

## 2. Liouville space formulation

### 2.1. Outline of the formalism

In this section, we re-derive the formal set of equations in Liouville space to calculate the steady-state density matrix. This necessarily includes a relaxation matrix; in the present case, we use a simple random-field mechanism, but more sophisticated relaxation can be incorporated easily. We can also include a continuous rf field, to calculate the CW spectrum for any values of the parameters. However, a much more powerful approach is to embed a pulse sequence into the formulation. The same formalism can then be used to calculate the steady-state created by a more complex pulse sequence with explicit pulses and delays. For this paper, we apply only the simple pulse–delay SSFP sequence, but there is nothing in the theory that restricts us to this experiment.

Table 1
Spherical tensor basis for the Liouville Space of a single spin-$\frac{1}{2}$

$|0) = \frac{1}{\sqrt{2}}\mathbf{1}$
$|1_{+1}) = -(\mathbf{I}_x + i\mathbf{I}_y)$
$|1_0) = \sqrt{2}\mathbf{I}_z$
$|1_{-1}) = (\mathbf{I}_x - i\mathbf{I}_y)$

For a single spin, the Liouville space description corresponds directly to the Bloch equations, and the calculations are easy. We use the computer algebra program Maple[1] to symbolically derive the CW solution. Next, we derive the symbolic SSFP solution, and show how the pulse flip angle and the delay are combined to provide the same effect as the CW field. This can be done exactly, or in an approximate fashion, in which the delay is assumed to be small compared to the relaxation times and the time associated with the offset between the rf and the Larmor frequency. This approximate solution converges to the CW solution, and represents the SSFP experiment.

For two spins, the calculation is considerably more difficult. As well as the rf power, we now must consider the chemical shift difference and the coupling constant. There are some approximate analytical calculations of the double-quantum intensity [26], which we are able to derive and extend symbolically. We also use Maple to explore this spectroscopy numerically, in order to get a feeling for how a coupled spin system responds. For three or more spins, symbolic calculations are out of the question, but numerical calculations are certainly feasible. Worvill [7] had looked at the response of a three-spin system, in order to test whether it was sensitive to the exact nature of the relaxation mechanism. Because we use a simpler relaxation model than Worvill, the spectra do not match exactly, but the basic resemblance is very strong.

The basic tool for these calculations is the density matrix. It encodes all possible information about a spin system and the measurements we can make to extract that information. We use the Liouville space method [28] to represent the density matrix and determine solutions of the continuous wave and pulsed NMR experiments.

[1] http://www.maplesoft.com/

In this paper, $|0\rangle, |1_{+1}\rangle, |1_0\rangle$ and $|1_{-1}\rangle$ represent the four observables for one single spin-$\frac{1}{2}$ system in the Liouville space, see Table 1, following the notation of Bain and Martin [28].

These observables form a basis for a single spin system,

$$\{|0\rangle, |1_{+1}\rangle, |1_0\rangle, |1_{-1}\rangle\}, \tag{1}$$

and combine to form bases for multiple spin-$\frac{1}{2}$ systems by using direct products of the single spin system basis.

The density operator is a vector in Liouville space and the equation of motion for the density matrix vectors is expressed as

$$\partial\rho/\partial t = -\mathrm{i}\mathcal{L}\rho - \mathcal{R}(\rho - \rho_{\mathrm{eq}}), \tag{2}$$

where $\rho$ is the state vector of the spin system and $\rho_{\mathrm{eq}}$ is the equilibrium state, $\mathcal{L}$ is the Liouvillian matrix encoding information about Larmor frequencies, chemical structure and couplings (if the spin system is multiple), and $\mathcal{R}$ is the relaxation matrix. Please note that $\mathrm{i}\mathcal{L}\rho_{\mathrm{eq}} = 0$.

In the Liouville space, observables are detected by taking the dot (scalar) product between two Liouville space vectors. This is equivalent to the trace product in the operator formalism [28,29], i.e.

$$(P|Q) = \mathrm{trace}(\hat{P}\hat{Q}), \tag{3}$$

where, on the left-hand side, $P$ and $Q$ are Liouville space vectors, whereas the right-hand side $\hat{P}$ and $\hat{Q}$ denote Hilbert space operators. We can only detect the single quantum signal, which is $|1_{+1}\rangle$ in our basis, representing the total $x$–$y$ magnetization precessing in the positive direction.

### 2.2. General solution for the continuous wave case

In continuous wave (CW) NMR experiments, a continuous radio frequency field, $B_1$, is applied, making the evolution

$$\partial\rho/\partial t = -\mathrm{i}(\mathcal{L} + \mathcal{B})\rho - \mathcal{R}(\rho - \rho_{\mathrm{eq}}), \tag{4}$$

where $\mathcal{B}$ is the matrix for the effect of the rf field $B_1$. The next section will give these matrices for a single spin system. Because $|0\rangle$, the total number of spins, is a constant, we only consider the parts $(|1_{+1}\rangle, |1_0\rangle$ and $|1_{-1}\rangle)$ of these matrices in the computation. These components represent the $x$–$y$ and $z$ magnetization.

At steady state,

$$\partial\rho/\partial t = 0. \tag{5}$$

Considering Eqs. (4) and (5), we get the general expression for calculating the steady state:

$$\rho_{\mathrm{SS}} = (\mathrm{i}(\mathcal{L} + \mathcal{B}) + \mathcal{R})^{-1}\mathcal{R}\rho_{\mathrm{eq}}. \tag{6}$$

We can solve the single spin system symbolically using Maple library functions. For two-spin systems, such general methods fail, and we have written our own Gaussian elimination procedures designed using knowledge of the structure of the Liouvillians to keep intermediate symbolic expressions from exploding. For arbitrary systems, we need to use numerical methods.

### 2.3. General solution for the pulsed case

We consider pulsed NMR experiments composed of hard pulses and delays. In the first case we can ignore precession and relaxation ($\mathcal{L} = \mathcal{R} = 0$), and in the second there is no rf field ($B_1 = 0$). We solve the corresponding reduced systems separately.

The effect of a hard pulse is equivalent to a rotation of the reference frame. A rotation for spherical tensors is defined by a Wigner rotation matrix [30] and the direct product provides the rotation for multiple spins. The following equation gives the effect of a hard pulse:

$$\rho_+ = W(\alpha)\rho_-, \tag{7}$$

where $\rho_-$ is the state before the pulse, $\rho_+$ is the state after the pulse, $W(\alpha)$ is the rotation matrix around the $y$-axis, $\alpha$ is the flip angle which is related to the strength of the radio frequency field $B_1$. Hard pulses correspond to the limit in which $\gamma B_1 \to \infty$ and pulse width $\to 0$, but the flip angle $\alpha$ remains constant.

For short delays, we have the following approximation:

$$\gamma B_1 \approx \frac{\alpha}{T_{\mathrm{R}}}, \tag{8}$$

where $T_{\mathrm{R}}$ is the delay time.

Fig. 1 displays the simplest steady state pulse sequence. At each time point, we can calculate the spin states $\rho_{\mathrm{a}}, \rho_{\mathrm{b}}, \rho_{\mathrm{c}}, \rho_{\mathrm{d}}$. When the spin system is at the steady state, $\rho_{\mathrm{a}} = \rho_{\mathrm{c}}$ and $\rho_{\mathrm{b}} = \rho_{\mathrm{d}}$. We can use equations for the spin dynamics to relate spin states in different repeat times, and then solve these equations for the steady-state value. In this paper, the measured signal is $\rho_{\mathrm{b}}$ which is corresponded to the echo signal in [22]. Gyngell [22] and Hanicke and Vogel [19] discuss the solution of a single spin system at the time point $a$ and $b$. In this paper, we give a general full expression and general approximate expression for an SSFP experiment on a system of $n$ spins.

In order to calculate the spin states at different time points, we need to solve Eq. (2). Considering the fact that $\mathrm{i}\mathcal{L}\rho_{\mathrm{eq}} = 0$, Eq. (2) can be reformulated as:

$$\frac{\mathrm{d}}{\mathrm{d}t}(\rho - \rho_{\mathrm{eq}}) = (-\mathrm{i}\mathcal{L} - \mathcal{R})(\rho - \rho_{\mathrm{eq}}). \tag{9}$$

So the principal solution of Eq. (2) is:

$$\rho(t) = \mathrm{e}^{-(\mathrm{i}\mathcal{L}+\mathcal{R})t}(\rho_0 - \rho_{\mathrm{eq}}) + \rho_{\mathrm{eq}}, \tag{10}$$

where $\rho_0$ is the state at time $t = 0$ which is the initial state when the delay starts.

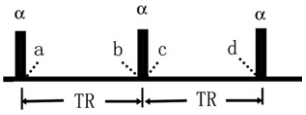


Fig. 1. The simplest pulsed NMR experiment.

Based on Fig. 1, the states $\rho_a, \rho_b$, and $\rho_c$ are related by affine equations:

$$\rho_b = e^{-(i\mathcal{L}+\mathcal{R})^{T_R}}(\rho_a - \rho_{eq}) + \rho_{eq} \tag{11}$$

$$\rho_c = W(\alpha)\rho_b, \tag{12}$$

where $T_R$ is the repeat time—the time between successive pulses.

Because $\rho_c$ is equal to $\rho_a$ at the steady state, solving Eqs. (11) and (12), we get the general analytic solution for SSFP experiments:

$$\rho_b = (\mathbf{1} - e^{-(i\mathcal{L}+\mathcal{R})T_R}W(\alpha))^{-1}(\mathbf{1} - e^{-(i\mathcal{L}+\mathcal{R})T_R})\rho_{eq}, \tag{13}$$

where $\mathbf{1}$ is an identity matrix which has the same size as the Liouvillian matrix and the relaxation matrix.

It is difficult to calculate $\rho_b$ symbolically for a multiple-spin system using Eq. (13). We will give the symbolic solution $\rho_b$ for a single-spin system and use Eq. (13) in the numerical computation for multiple-spin systems.

In order to analyze SSFP and discover the relationship between parameters such as the repeat time, relaxation times, Larmor frequencies, and others, we use the following equation to approximately calculate $\rho_b$ when the repeat time of pulses is very short:

$$\partial\rho/\partial t \approx \frac{\rho_b - \rho_a}{T_R}. \tag{14}$$

Replacing the left side of Eq. (2), we get a new equation:

$$\frac{\rho_b - \rho_a}{T_R} \approx -i\mathcal{L}\rho_b - \mathcal{R}(\rho_b - \rho_{eq}). \tag{15}$$

Solving Eqs. (15) and (12), $\rho_b$ is expressed:

$$\rho_b \approx T_R(\mathbf{1} + (i\mathcal{L} + \mathcal{R})T_R - W(\alpha))^{-1}\mathcal{R}\rho_{eq}. \tag{16}$$

The above equation is the general approximate expression for an SSFP experiment on a system of $n$ spins. Comparing Eqs. (13) and (16) , it is cheaper to calculate $\rho_b$ using Eq. (16) which does not require the computation of the exponential of a complex matrix.

## 3. Solutions of a single spin-$\frac{1}{2}$ system

First, we list each matrix for a single spin system in our calculation. All of these matrices are constructed in the basis Eq. (1).

The Liouvillian matrix of a single spin-$\frac{1}{2}$ system is:

$$\mathcal{L} = \begin{pmatrix} 0 & 0 & 0 & 0 \\ 0 & \Delta\omega & 0 & 0 \\ 0 & 0 & 0 & 0 \\ 0 & 0 & 0 & -\Delta\omega \end{pmatrix} \tag{17}$$

where $\Delta\omega$ is the resonance offset $(\omega - \omega_0)$, and $\omega_0$ is the center frequency.

The relaxation matrix of a single spin-$\frac{1}{2}$ system is:

$$\mathcal{R} = \begin{pmatrix} 0 & 0 & 0 & 0 \\ 0 & \frac{1}{T_2} & 0 & 0 \\ 0 & 0 & \frac{1}{T_1} & 0 \\ 0 & 0 & 0 & \frac{1}{T_2} \end{pmatrix} \tag{18}$$

where $T_1$ and $T_2$ are the spin–lattice and spin–spin relaxation times.

The $\mathcal{B}$ matrix for the effect of CW acting on a single spin-$\frac{1}{2}$ system along the $x$-axis is:

$$\mathcal{B} = \begin{pmatrix} 0 & 0 & 0 & 0 \\ 0 & 0 & -\frac{1}{\sqrt{2}}\gamma B_1 & 0 \\ 0 & -\frac{1}{\sqrt{2}}\gamma B_1 & 0 & \frac{1}{\sqrt{2}}\gamma B_1 \\ 0 & 0 & \frac{1}{\sqrt{2}}\gamma B_1 & 0 \end{pmatrix} \tag{19}$$

where $\gamma$ is the gyromagnetic ratio and $B_1$ is the strength of the radio-frequency.

The rotation matrix, which rotates around the $y$-axis, for the effect of a pulse acting on a single spin-$\frac{1}{2}$ system in the Liouville space is:

$$W(\alpha) = \begin{pmatrix} 1 & 0 & 0 & 0 \\ 0 & (\cos(\alpha/2))^2 & \frac{1}{\sqrt{2}}\sin(\alpha) & (\sin(\alpha/2))^2 \\ 0 & -\frac{1}{\sqrt{2}}\sin(\alpha) & \cos(\alpha) & \frac{1}{\sqrt{2}}\sin(\alpha) \\ 0 & (\sin(\alpha/2))^2 & -\frac{1}{\sqrt{2}}\sin(\alpha) & (\cos(\alpha/2))^2 \end{pmatrix} \tag{20}$$

where $\alpha$ is the flip angle.

All of matrices $\mathcal{L}, \mathcal{R}, \mathcal{B}$ and $W$ are 4-by-4 which corresponds to the basis Eq. (1). As we said before, in order to avoid singular matrices, we only consider the subspace spanned by $\{|1_{+1}), |1_0), |1_{-1})\}$ in the computation. In general, when we set up multiple spin-$\frac{1}{2}$ systems, we need to take direct-products of 4-by-4 matrices first, before eliminating the total magnetization component. Often, the equilibrium is given as:

$$\rho_{eq} = \begin{pmatrix} 0 \\ 1 \\ 0 \end{pmatrix}$$

but in this paper, we use

$$\rho_{eq} = \begin{pmatrix} 0 \\ \sqrt{2}M_0 \\ 0 \end{pmatrix}$$

to facilitate symbolic comparisons between CW and SSFP.

### 3.1. Single-spin CW solution

Substituting the matrices in Eqs. (17)–(19) for a single spin system into Eq. (6), and applying the detection method from Eq. (3), we get the measured signal $s$ in the $x$–$y$ plane:

$$s = M_0 \frac{\gamma B_1 (\Delta\omega T_2 + \mathrm{i}) T_2}{1 + (\Delta\omega)^2 T_2^2 + (\gamma B_1)^2 T_1 T_2}, \tag{21}$$

which has real and imaginary parts:

$$s_{\mathrm{re}} = M_0 \frac{\gamma B_1 T_2^2 \Delta\omega}{1 + (\Delta\omega)^2 T_2^2 + (\gamma B_1)^2 T_1 T_2} \tag{22}$$

$$s_{\mathrm{im}} = M_0 \frac{\gamma B_1 T_2}{1 + (\Delta\omega)^2 T_2^2 + (\gamma B_1)^2 T_1 T_2}. \tag{23}$$

Eqs. (22) and (23) are the measured signal from a single spin system at steady state in a continuous wave NMR experiment. This solution can also be directly computed using the Bloch equations [31].

### 3.2. Solution of a single-spin system of pulsed NMR experiments

Replacing Eq. (13) with the matrices in Eqs. (17), (18), and (20) for a single spin system, and applying the detection method from Eq. (3), we get the measured signal $s$ at the time point $b$ in the $x$–$y$ plane. Note that, in this case, $B_1$ is along the $y$-axis rather than the $x$-axis and the absorption mode spectra will be the real part of the complex signal.

$$s_{\mathrm{re}} = M_0 \frac{\mathrm{e}^{-\frac{T_R}{T_2}}\left(1 - \mathrm{e}^{-\frac{T_R}{T_1}}\right)\sin(\alpha)\left(\cos(T_R\Delta\omega) - \mathrm{e}^{-\frac{T_R}{T_2}}\right)}{Q_1} \tag{24}$$

$$s_{\mathrm{im}} = -M_0 \frac{\mathrm{e}^{-\frac{T_R}{T_2}}\left(1 - \mathrm{e}^{-\frac{T_R}{T_1}}\right)\sin(\alpha)\sin(T_R\Delta\omega)}{Q_1}, \tag{25}$$

where,

$$Q_1 = 1 - \mathrm{e}^{-\frac{T_R}{T_1}}\cos(\alpha) - \mathrm{e}^{-\frac{2T_R}{T_2}}\left(\mathrm{e}^{-\frac{T_R}{T_1}} - \cos(\alpha)\right) - \mathrm{e}^{-\frac{T_R}{T_2}}\left(1 - \mathrm{e}^{-\frac{T_R}{T_1}}\right)(1 + \cos(\alpha))\cos(T_R\Delta\omega).$$

Using Eq. (12), we obtain the same magnetization at time point $a$ given by Gyngell [22]. These equations are the full solution for the steady state of pulsed NMR experiments. Note that for each repeat time, the signal is periodic in $\Delta\omega$ with period $1/T_R$.

Substituting the matrices from Eqs. (17), (18), and (20) for a single spin system into Eq. (16), and applying the detection method from Eq. (3), we get the approximate measured signal at the time point $b$ in the $x$–$y$ plane:

$$s_{\mathrm{re}} = M_0 \times \frac{\sin(\alpha) T_R T_2}{T_R^2 + T_R^2 (\Delta\omega)^2 T_2^2 + Q_2} \tag{26}$$

$$s_{\mathrm{im}} = -M_0 \times \frac{\sin(\alpha) T_R \Delta\omega T_2^2}{T_R^2 + T_R^2 (\Delta\omega)^2 T_2^2 + Q_2,} \tag{27}$$

where

$$Q_2 = \left(4T_1T_2 + 2T_R(T_1 + T_2) + 2T_1T_2^2T_R(\Delta\omega)^2\right)(\sin(\alpha/2))^2.$$

Eqs. (24)–(27) apply for all flip angles used in SSFP experiments. Carr [4] plots some approximate diagrams when flip angles are over $\pi/12$ radians.

In order to observe the relation between CW and SSFP solutions, we explore the situation in which the flip angle is very small. In this case, $\sin(\alpha) \approx \alpha$ and $\sin(\alpha/2) \approx \alpha/2$. Considering the relationship, Eq. (8), between the flip angle $\alpha$ and the radio-frequency $B_1$ field, we get the approximate equations for the signal.

$$s_{\mathrm{re}} \approx M_0 \times \frac{\gamma B_1 T_2}{1 + (\Delta\omega)^2 T_2^2 + (\gamma B_1)^2 T_1 T_2 + Q_3} \tag{28}$$

$$s_{\mathrm{im}} \approx -M_0 \times \frac{\gamma B_1 \Delta\omega T_2^2}{1 + (\Delta\omega)^2 T_2^2 + (\gamma B_1)^2 T_1 T_2 + Q_3}, \tag{29}$$

where,

$$Q_3 = \frac{1}{2}(\gamma B_1)^2 T_R (T_1 + T_2 + T_1 T_2^2 (\Delta\omega)^2).$$

Comparing Eqs. (22) and (29), and Eqs. (23) and (28), if

$$T_R \ll \min\left(\frac{2}{T_1(\gamma B_1)^2}, \frac{2T_1T_2}{T_1 + T_2}\right) \tag{30}$$

the factor $Q_3$ which broadens the signal can be ignored, Eqs. (28) and (29) will become the same as Eqs. (23) and (22). The real and imaginary parts are swapped because, in this case, the rotation matrix rotates around the $y$-axis, while the $\mathcal{B}$ matrix acts on the spin system along the $x$-axis. From the condition on $T_R$, we derive the condition,

$$\alpha \ll \frac{2}{T_1 \gamma B_1}, \tag{31}$$

on the flip angle.

Thus far, solutions for the steady state magnetization in continuous wave and pulsed experiments have been given. The possibility of approximating CW NMR experiments with pulsed steady state experiments for single spin-$\frac{1}{2}$ systems has been explored. Under some conditions, the simulation is very close to the CW NMR experiments. In the next section, we analyze multiple-spin systems.

## 4. Double-quantum transitions of a 2-spin system

In this section, double-quantum transitions for coupled spin systems in steady state are discussed. In the Liouville formalism, double-quantum coherence of a 2-spin system is detectable. The double-quantum transitions can be obtained by observing the signal of the single quantum transitions at the frequency of $(\omega_A + \omega_B)/2$. In this section, we compare different methods of calculating double quantum transitions.

In the previous section, the matrices and vectors for a 1-spin system are listed. Matrices for a 2-spin system can be constructed based on the single spin system. A software package in Maple has been developed to build matrices and vectors for arbitrary spin systems. In this paper, we do not write out the matrices.

### 4.1. Symbolic solution of continuous wave experiments

The size of a full basis for a 2-spin system is 16. We do not consider the total magnetization, $|0)|0)$, component,

reducing the dimensions of the corresponding matrices $\mathcal{L}, \mathcal{B}, \mathcal{R}$ to $15 \times 15$.

Eq. (6) is used to calculate the steady state of CW experiments, but it is difficult to directly compute symbolic $\rho_{ss}$ for a 2-spin system. Maple library functions could not compute a simplified expression, because it was too large. However, forcing simplification at each step of (hand-coded) Gaussian elimination used to solve the system does produce a useful answer.

The following method is used to get the strength of the double quantum transitions of a 2-spin system. The signal $\rho_{ss}$ can be separated into real ($\rho_r$) and imaginary ($\rho_i$) parts. After which the evolution equation

$$(\mathcal{R} + \mathrm{i}(\mathcal{L} + \mathcal{B}))(\rho_r + \mathrm{i}\rho_i) = \mathcal{R}\rho_{eq} \tag{32}$$

similarly separates:

$$\mathcal{R}\rho_r - (\mathcal{L} + \mathcal{B})\rho_i = \mathcal{R}\rho_{eq} \tag{33}$$

$$(\mathcal{L} + \mathcal{B})\rho_r + \mathcal{R}\rho_i = 0. \tag{34}$$

All of the entries of $\rho_{eq}$ are real numbers, so $\rho_{eq}$ represents a real vector. And all of components of the matrices and vectors of the above equations are real. Solving the two equations, we get the following two linear systems:

$$(\mathbf{1} + \mathcal{R}^{-1}(\mathcal{L} + \mathcal{B})\mathcal{R}^{-1}(\mathcal{L} + \mathcal{B}))\rho_r = \rho_{eq} \tag{35}$$

$$(\mathbf{1} + \mathcal{R}^{-1}(\mathcal{L} + \mathcal{B})\mathcal{R}^{-1}(\mathcal{L} + \mathcal{B}))\rho_i = -\mathcal{R}^{-1}(\mathcal{L} + \mathcal{B})\rho_{eq} \tag{36}$$

On the other hand, considering the detection of a 2-spin system, we only need the observable (first and fourth, in our basis) components of $\rho_{ss}$ to get the signal of double quantum transitions, so we do not need to get the whole solution of $\rho_{ss}$. At the same time, the signal of double quantum transitions of a 2-spin system will be at the frequency $(\omega_A + \omega_B)/2$ which means that the value of $\Delta\omega$ is 0 in the Liouville matrix $\mathcal{L}$.

A Maple procedure was developed to implement manual Gaussian elimination to solve the new linear systems. Due to the fact that we need only the first and fourth elements, it makes sense to start the Gaussian elimination at the end of the matrix, the 15th element. For each step, the pivot was chosen by inspection of the matrix elements, and the Gaussian elimination proceeded. Using this procedure, the signals of double quantum transitions of a 2-spin system in CW experiments ($B_1$ is along the $x$-axis.) are:

$$s_{re} = 0 \tag{37}$$

$$s_{im} = M_0 \frac{8T_2\gamma B_1(E_1(\gamma B_1)^2 + T_1^2T_2^2\delta^2 + E_5)}{T_1^2T_2^4\delta^4 + E_2\delta^2 + E_3(\gamma B_1)^4 + E_4(\gamma B_1)^2 + 4E_5}, \tag{38}$$

where,

$$E_1 = 2T_1T_2^2E_6$$

$$E_2 = 8T_1T_2^3 + 8T_1^2T_2^2 + 2T_1T_2^3(2T_1^2 + T_1T_2 + T_2^2)(\gamma B_1)^2 + 4T_2^4$$

$$E_3 = 4T_1T_2E_1$$

$$E_4 = 8T_1T_2(2T_1^2 + 3T_2^2 + 5T_1T_2 + T_1T_2^2(2T_1 + 3T_2)J^2)$$

$$E_5 = 4(T_1 + T_2)E_6$$

$$E_6 = T_1T_2^2J^2 + T_1 + T_2,$$

where $J$ is the coupling constant of spin A and spin B; $\delta$ is the difference of Larmor frequencies of spin A and spin B; spin A and spin B have same relaxation times $T_1$ and $T_2$. Yatsiv [26] gives the approximate expression, but Eq. (38) is a full solution. Based on this equation, it is easily to observe the relationship of the double quantum transitions with these factors such as the coupling constant, the strength of the rf field, the relaxation times.

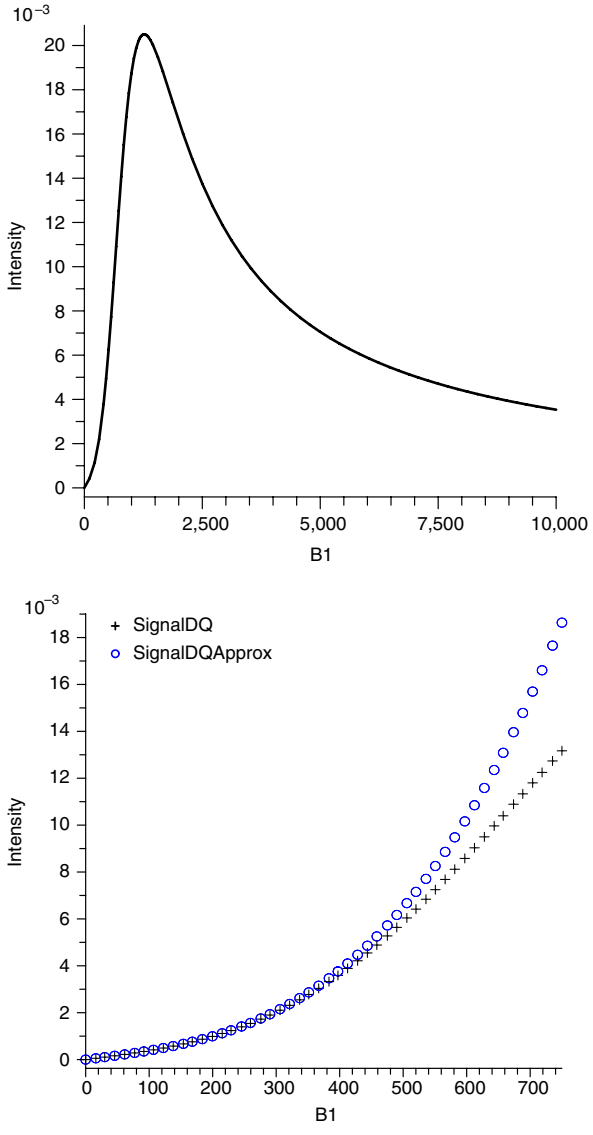


Fig. 2. The intensity of the double quantum transition at the frequency $\frac{\omega_A+\omega_B}{2}$ is a function of $B_1$. Parameters: $\delta_{AB} = 1500$ Hz, $T_1 = 0.04$ s, $T_2 = 0.02$ s, $J = 183$ Hz.

When the coupling constant $J$ is 0, according to Eq. (38), the signal of the double quantum transition is:

$$s_{\text{imag},J=0} = M_0 \frac{2\gamma B_1 T_2}{1 + T_1 T_2 (\gamma B_1)^2 + (\delta T_2/2)^2} \tag{39}$$

which is the sum of signal of the wings of two independent spin systems at the midpoint between them. When the coupling constant $J$ is going to the infinity, the signal will be:

$$s_{\text{imag},J=\infty} = M_0 \frac{2\gamma B_1 T_2}{1 + T_1 T_2 (\gamma B_1)^2} \tag{40}$$

which is the same as the signal when $\delta = 0$.

When $B_1$ is zero, the signal will be 0. When $B_1$ tends toward infinity, saturation will appear and the signal will also be 0. Fig. 2 shows the trend.

When substituting $J, T_1, T_2$ and $\delta$ with the parameters of Fig. 2 to Eq. (38), the intensity of the double quantum transition is a function of the variable $B_1$ as the following:

$$\text{SignalDQ} = \frac{7.680101 \times 10^{-5} B_1^3 + 7.007729 B_1}{2020634.314 + 0.269143 B_1^2 + 2.172261 \times 10^{-6} B_1^4}. \tag{41}$$

When $B_1$ is small, the intensity could be approximate by a cubic function:

$$\text{SignalDQApprox} = 3.800837 \times 10^{-11} B_1^3 + 3.468084 \times 10^{-6} B_1. \tag{42}$$

When $\delta$ is zero, the intensity will be:

$$s_{\text{imag},\delta=0} = M_0 \frac{2\gamma B_1 T_2}{1 + T_1 T_2 (\gamma B_1)^2}. \tag{43}$$

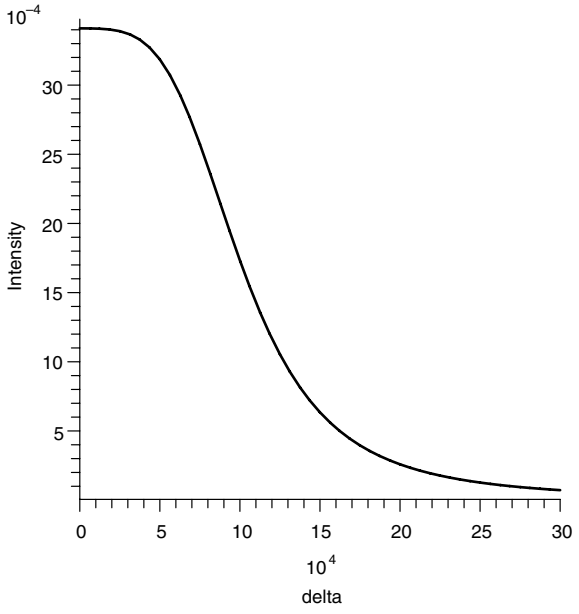


Fig. 3. The intensity of the double quantum transition is a function of $\delta$. Parameters: $\gamma B_1 = 1650$ Hz, $T_1 = 0.04$ s, $T_2 = 0.02$ s, $J = 183$ Hz.

When $\delta$ tends toward infinity, the intensity will also tend toward zero. Fig. 3 shows the trend.

Using numerical computation, spectrum can be plotted out by functions Eqs. (6) and (3). The spectra of CW experiments (Figs. 4 and 5) are plotted out as a function of rf field and coupling constant so as to show the broadening phenomena.

Calculations using the pulsed NMR can also be used to observe the signal at the frequency $\frac{\omega_A+\omega_B}{2}$ by computing Eqs. (13) and (16). The results (not shown) confirm that the results of SSFP are very close to CW experiments under small flip angle conditions.

## 5. Extension to multiple spin-$\frac{1}{2}$ systems

Eqs. (6), (13) and (16) give the general solutions of multiple spin-$\frac{1}{2}$ systems. These equations can be applied to explore the spectrum, multiple quantum transitions, design

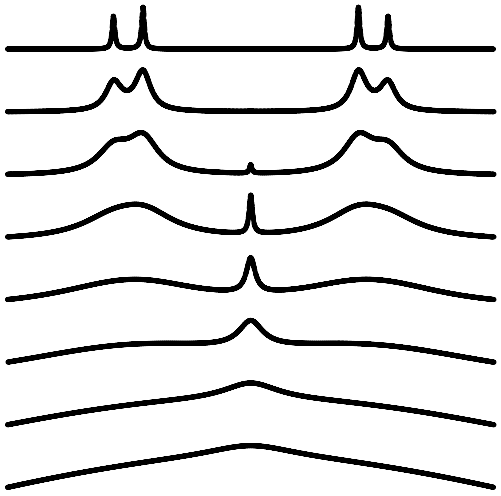

Fig. 4. The spectra of a coupled spin system with different $B1$. Parameters: $\delta_{AB} = 1500$ Hz, $T_1 = 0.04$ s, $T_2 = 0.02$ s, $J = 183$ Hz, $\gamma B_1 = 0.043, 43, 86, 172, 344, 688, 1376, 2173$ Hz.

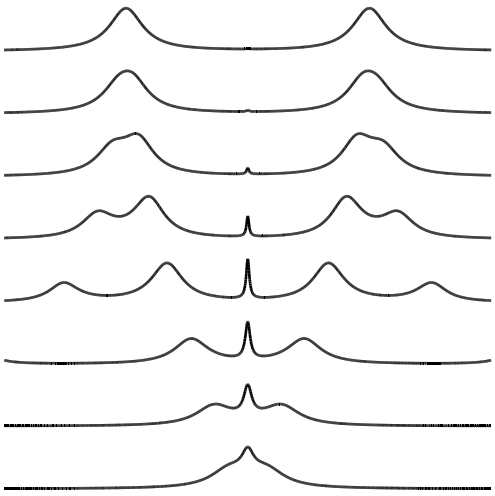

Fig. 5. The spectra of a coupled spin system with different coupling constants. Parameters: $\delta_{AB} = 1500$ Hz, $T_1 = 0.04$ s, $T_2 = 0.02$ s, $\gamma B_1 = 86$ Hz, $J = 0, 80, 160, 320, 640, 1280, 2560, 5120$ Hz.

of pulse sequences, optimization problems. This section shows the feasibility and cost to handle multiple spin systems by the Maple package.

Worvill calculated the saturation spectra of a three-spin system using various models of the spin relaxation. In our case, we have just used the simple random-field model, so the spectra in Fig. 6 do not exactly match Worvill's figures (Figs. 1–8) [7]. However, the resemblance is close enough to validate our method.

When calculating one point of the steady state, Eq. (6) needs to compute a complex matrix inverse one time and the multiplication of a complex matrix and a vector two

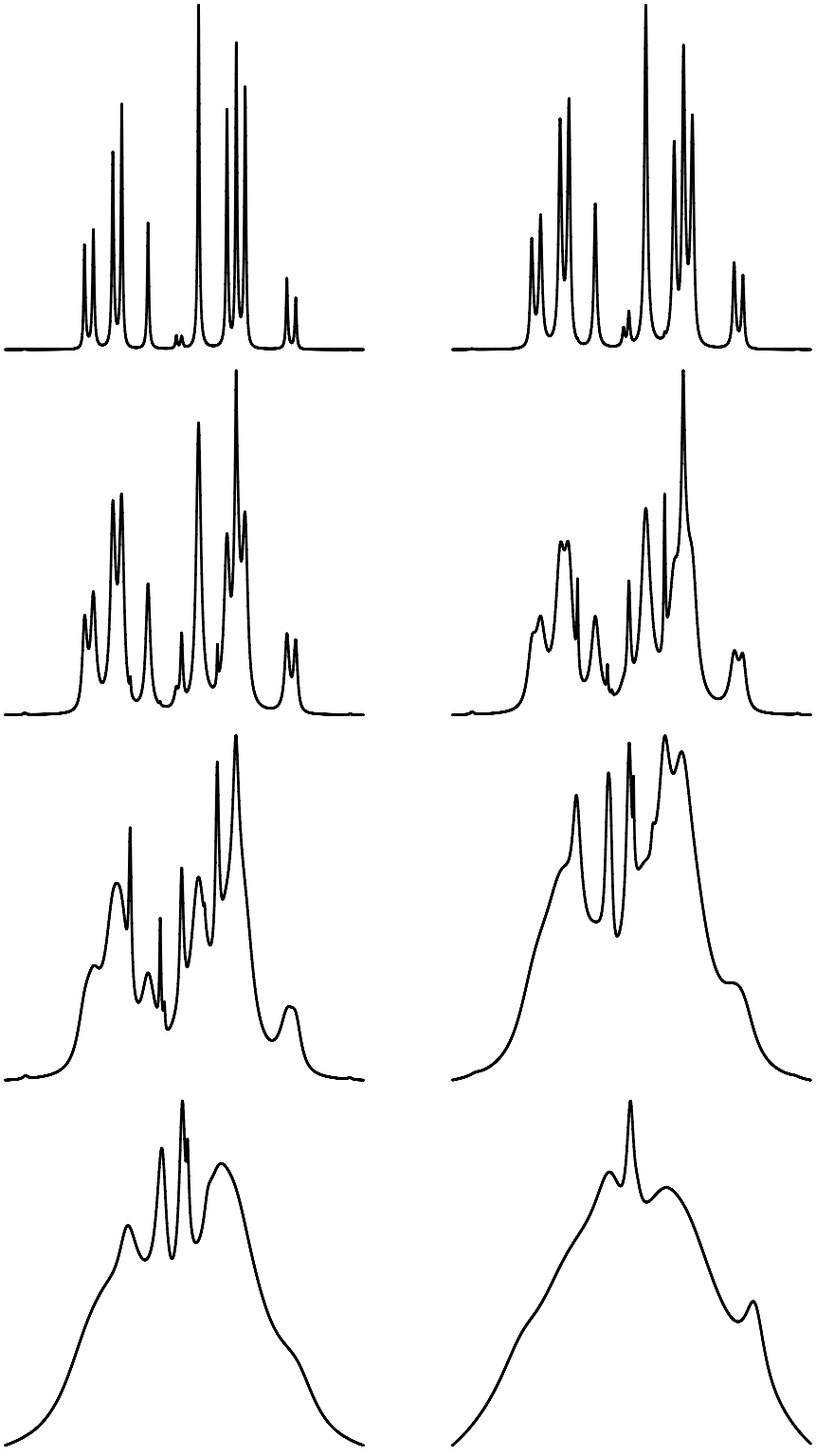

Fig. 6. Reproducing Worvill's figures (Figs. 1–8) which are spectrum of a 3-spin system [7] with different $B_1$. Parameters: $\omega_A = 634.05$ Hz, $\omega_B = 613.36$ Hz, $\omega_C = 583.82$ Hz, $J_{AB} = 17.38$ Hz, $J_{AC} = 1.57$ Hz, $J_{BC} = 10.50$ Hz, $T_1 = 1$ s, $T_2 = 1$ s, $B_1 = 0.1, 10, 20, 40, 70, 150, 250, 500$ nT.

Table 2
CPU time (s) of calculating $1k$ points for 3-, 4-, 5-spin systems

| System | CW method | SSFP accurate method | SSFP approximate method |
|---|---|---|---|
| 3-spin | 56 | 190 | 160 |
| 4-spin | 575 | 3841 | 2897 |
| 5-spin | 10,031 | 102,586 | 52,483 |

times; Eq. (13) needs to compute an exponential of a complex matrix one time, the multiplication of a complex matrix and a vector two times, and the addition of matrices two times; Eq. (16) has the same cost as Eq. (6) plus two times' addition of matrices. The computational complexity grows quickly in the Liouville space , since the dimension of the matrices or the eigenvalues for a system of size is $4^n$. Table 2 shows the cost for 3-, 4-, and 5-spin systems.

## 6. Conclusions

In this paper, we have described and tested a formalism for treating steady-state methods. One of the best tests is to reproduce a number of CW experiments, but the method is not restricted to this limit. The symbolic solutions of steady state for the single spin system are given. The double quantum transitions of continuous wave experiments is also calculated out by the algebraic computation. A series of spectrum for multiple spin systems are plotted out by different ways. All of these things show that steady state pulsed NMR approximates CW experiments well. The flexibility of our Maple tools [2] allow us to explore more complicated spin systems with more sophisticated pulse sequences. Along with the increase of number of spins, the computational complexity grows quickly, so some numerical methods such as BLAS, sparse matrix technique should be applied to improve the efficiency. However, the method has proved itself, so future work will apply it to more complex systems.

## Acknowledgments

Alex D. Bain thanks the Natural Science and Engineering Research Council of Canada (NSERC) for financial support.

## References

[1] J. Keeler, Understanding NMR Spectroscopy, John Wiley, New York, 2005.
[2] M.H. Levitt, Spin Dynamics: Basics of Nuclear Magnetic Resonance, John Wiley and Sons, New York, 2001.
[3] R.R. Ernst, G. Bodenhausen, A. Wokaun, Principles of Nuclear Magnetic Resonance in One and Two Dimensions, Clarendon Press, Oxford University Press, New York, 1987.
[4] H.Y. Carr, Steady-state free precession in nuclear magnetic resonance, Phys. Rev. 112 (5) (1958) 1693–1701.
[5] J.I. Kaplan, S. Meiboom, Double-quantum transitions in nuclear magnetic resonance spectra of liquids, Phys. Rev. 106 (3) (1957) 499–501.
[6] W.A. Anderson, R. Freeman, C.A. Reilly, Assignment of NMR spectra with the aid of double-quantum transitions, J. Chem. Phys. 39 (6) (1963) 1518–1531.
[7] K.M. Worvill, The NMR multiple quantum spectrum of a three-spin system, J. Magn. Reson. 18 (1975) 217–229.
[8] P. Guntert, N. Schaefer, G. Otting, K. Wuthrich, POMA: a complete mathematica implementation of the NMR product–operator formalism, J. Magn. Reson. A 101 (1) (1993) 103–105.
[9] A. Jerschow, MathNMR: spin and spatial tensor manipulations in Mathematica, J. Magn. Reson. 176 (1) (2005) 7–14.
[10] I. Rodriguez, J. Ruiz-Cabello, Density matrix calculations in Mathematica™, Concepts Magn. Reson. 13 (2) (2001) 143–147.
[11] J.W. Shriver, NMR product–operator calculations in mathematica, J. Magn. Reson. 94 (1991) 612–616.
[12] S.Z. Ageev, P.P. Man, B.C. Sanctuary, Detection of double and four quantum coherences for spin excited by spin lock pulse sequences, J. Magn. Reson. 128 (1) (1997) 12–20.
[13] M.P. Barnett, J.F. Capitani, J. von zur Gathen, J. Gerhard, Symbolic calculation in chemistry: selected examples, Int. J. Quant. Chem. 100 (2) (2004) 80–104.
[14] D.J. Isbister, M.S. Krishnan, B.C. Sanctuary, Use of computer algebra for the study of quadrupole spin systems, Mol. Phys. 86 (6) (1995) 1517–1535.
[15] R. Freeman, H.D.W. Hill, Phase and intensity anomalies in fourier transform NMR, J. Magn. Reson. 4 (3) (1971) 366–383.
[16] P. Waldstein, W.E. Wallace Jr., Driven equilibrium methods for enhancement of nuclear transients, Rev. Sci. Instrum. 42 (4) (1971) 437–440.
[17] C. Ganter, Steady state of gradient echo sequences with radiofrequency phase cycling: analytical solution, contrast enhancement with partial spoiling, Magn. Reson. Med. 55 (1) (2006) 98–107.
[18] E.M. Haacke, R.W. Brown, M.R. Thompson, R. Venkatesan, Magnetic Resonance Imaging: Physical Principles and Sequence Design, Wiley-Liss, New York, 1999.
[19] W. Hänicke, H.U. Vogel, An analytical solution for the SSFP signal in MRI, Magn. Reson. Med. 49 (4) (2003) 771–775.
[20] B.A. Hargreaves, S.S. Vasanawala, J.M. Pauly, D.G. Nishimura, Characterization and reduction of the transient response in steady-state MR imaging, Magn. Reson. Med. 46 (1) (2001) 149–158.
[21] W.S. Hinshaw, Image formation by nuclear magnetic resonance: the sensitive-point method, J. Appl. Phys. 47 (8) (1976) 3709–3721.
[22] M.L. Gyngell, The steady-state signals in short-repetition-time sequences, J. Magn. Reson. 81 (3) (1989) 474–483.
[23] K. Scheffler, A pictorial description of steady-states in rapid magnetic resonance imaging, Concepts Magn. Reson. 11 (5) (1999) 291–304.
[24] J.I. Musher, Role of multiple quantum transitions in NMR: a three-spin system, J. Chem. Phys. 40 (4) (1964) 983–990.
[25] G. Bodenhausen, Multiple-quantum NMR, Prog. Nucl. Magn. Reson. Spectrosc. 14 (3) (1980) 137–173.
[26] S. Yatsiv, Multiple-quantum transitions in nuclear magnetic resonance, Phys. Rev. 113 (6) (1959) 1522–1537.
[27] C.K. Anand, A.D. Bain, Z. Nie, The simulation and optimization of pulsed NMR experiments using a liouville space method, in: The Maple Conference, Waterloo,Canada, 2006, pp. 123–135.
[28] A.D. Bain, J.S. Martin, FT NMR of nonequilibrium states of complex spin systems. I. A Liouville space description, J. Magn. Reson. 29 (1) (1978) 125–135.
[29] U. Fano, in: E.R. Caianiello (Ed.), Lectures on the Many-Body Problem, vol. 2, Academic Press, New York, 1964.
[30] R.N. Zare, Angular Momentum: Understanding Spatial Aspects in Chemistry and Physics, Wiley, New York, 1988.
[31] A. Carrington, A.D. McLachlan, Introduction to Magnetic Resonance with Applications to Chemistry and Physics, Harper and Row, New York, 1967.

[2] Copies of the Maple worksheet are available from Dr. Anand's website: http://www.cas.mcmaster.ca/~anand/index.html.